The band structure and Fermi surface of calcium

J. Phys. F: Metal Phys., 1971, Vol. 1. Printed in Great Britain

The band structure and Fermi surface of calcium

S. L. ALTMANN, A. R. HARFORD† and R. G. BLAKE
Department of Metallurgy, University of Oxford, UK
MS. received 23rd March 1971

Abstract. The conduction bands for Ca have been computed with a Slater-type potential and it is found that for less than 20% or more than 75% of the exchange term there is no overlap between the first and second band. The conduction and core bands, density of states, Fermi energy and Fermi surface are computed for an optimum value of the exchange. It is found that the Fermi surface is connected and agreement with all the known results of the de Haas–van Alphen effect is obtained. Although this is in apparent disagreement with the results of Vasvári *et al.* who obtain an unconnected Fermi surface, their Fermi level was wrongly located and when the error is corrected a connected surface should almost certainly be obtained. The effect of pressure on the Fermi surface and conductivity of Ca is discussed.

1. Introduction

The band structure of calcium was computed in this department in 1963 (Altmann and Cracknell 1964, Cracknell 1964) with the surprising result that, contrary to the free-electron prediction, the Fermi surface was small and disconnected, consisting of small pockets of holes in the first band and pockets of electrons in the second. It was also found that, when the lattice is compressed, the Fermi surface contracts down until it reaches a negligible size: Altmann and Cracknell (1964) suggested that anomalies in the electrical conductivity of Ca would thereby arise at high pressure. This prediction was verified by the results of Stager and Drickamer (1963) which came out almost at the same time. Dr. Bela Vasvári continued this work, first in this department and then independently, using a model potential (Vasvári *et al.* 1967) and confirmed substantially the description given above. There were nevertheless two differences. The first is purely semantic. When the calcium bands are computed one finds a crossing point between the first and second bands at Q, (a point of LW) which entails the existence of a line of degeneracy between those bands so that a gap between them cannot be established. Vasvári and Heine (1967) pointed out therefore that the material can become a semimetal but not a semiconductor, which appeared to contradict the work of Altmann and Cracknell (1964), who had suggested that Ca might become a semiconductor at high pressures. However, Altmann and Cracknell followed the practice, frequent at that time, and explicitly adopted by Drickamer (1965, p. 37), of referring to semimetals as well as semiconductors with the latter name. Their computations, of course, show the crossing point at Q (see Cracknell 1964) and their interpretation, if not their vocabulary, coincided with that adopted by Vasvári *et al.*

The second difference between the computations of Vasvári *et al.* and those of Altmann and Cracknell is a real one. Not unnaturally, since the potential fields used were different, the position of the pockets of holes varies from W for Vasvári *et al.* to K (see figure 7 for the position of these points) for Altmann and Cracknell (1964). We have now studied in great detail the effect of the potential field on the band structure of Ca and have found that the bands are extremely sensitive to the potential. It now appears that, if the Fermi surface were disconnected, the holes would be sited at W. However, we have found it impossible to construct a disconnected Fermi surface with holes at W that keeps the exact balance between the number of electrons in the second band and the number of holes in the first. We have

† Now with Burroughs Machines Ltd., City Wall House, Finsbury Street, London EC2.

also found that the results of Vasvári *et al.* appear to be in error in this respect and that the bands that they computed would lead to a connected Fermi surface. The connected Fermi surface which is given by our computations agrees in every detail with the experimental results of Condon and Marcus (1964) on the de Haas–van Alphen effect.

2. Method: interpolation

A general description of the cellular method of computation that we use is given by Altmann *et al.* (1968), who show that the results of the present method agree with those of the augmented plane wave method and the Green function method to 0·002 Ryd. However, we should like to correct two of the results published in that paper. As shown in it, the empty lattice eigenvalues for all symmetry points in $\boldsymbol{k}$ space are correct to 0·00001 Ryd, with a single error of 0·0001 Ryd. On the other hand, for general $\boldsymbol{k}$ values two errors were found between 0·01 and 0·02 Ryd, for expansions up to $l = 6$. The programme has been streamlined and higher values of l can now be used without difficulty for general points. The new results are shown in table 1 where they are compared with the old ones. It can be seen that the new errors are around 0·0003 Ryd, although they pertain to high energy bands.

Table 1. Empty fcc lattice eigenvalues (in Ryd)

Band	Exact eigenvalue	Calculated $l = 6$	Calculated $l = 8$
5	2·75	2·762861	2·749796
6	3·55	3·569161	3·550307

$\boldsymbol{k} = (0{\cdot}2, 0{\cdot}3, 0{\cdot}4)$. The lattice constant is 2π.

In order to obtain the density of states curves, the Fermi energy and a preliminary form of the Fermi surface, the eigenvalues are computed over a basic grid of the Brillouin zone and interpolated for about 5000 values of $\boldsymbol{k}$ in the basic region of it (1/48 of the Brillouin zone). A number of elaborate interpolation procedures have been proposed in the last few years but, owing to the fact that we are able to obtain very accurate eigenvalues over a fairly close grid, we find that a simple geometrical method, along the lines described by Altmann and Bradley (1965) gives excellent accuracy, as shown in table 2. A small random sample of interpolated eigenvalues for a Ca potential is shown in the table, computed with a basic grid of 95 points over 1/48 of the Brillouin zone. The largest error in the table is 0·003 Ryd and from over a hundred eigenvalues similarly examined we are confident that the interpolation programme that we have devised should nowhere give errors in excess of 0·005 Ryd.

Table 2. Eigenvalues (in Ryd) for Ca.

$(2\pi)^{-1} \times \boldsymbol{k}$ vector			Computed value	Interpolated
0·45	0·45	0·46	0·2252	0·2222
0·36	0·36	0·60	0·2651	0·2651
0·30	0·30	0·40	0·1470	0·1481
0·36	0·36	0·40	0·1674	0·1706
0·25	0·25	0·40	0·1368	0·1361
0·08	0·08	0·12	0·0140	0·0151
0·28	0·16	0·31	0·1047	0·1032

$a = 10{\cdot}5$ au

3. The potential fields

The potential field was obtained by the usual Mattheiss (1964) prescription (see Loucks 1967), starting from a complete SCF calculation with exchange for neutral Ca. The only difference in our case was that the full potential was taken throughout the cell rather than constructing a muffin tin potential. The Slater exchange term, $-6\alpha(3\rho/8\pi)^{1/3}$ was introduced, where ρ is the electronic density and α a weighting factor going from 0 to 1. In figure 1 the potentials used are shown for $\alpha = 0$, 0·4 and 1.

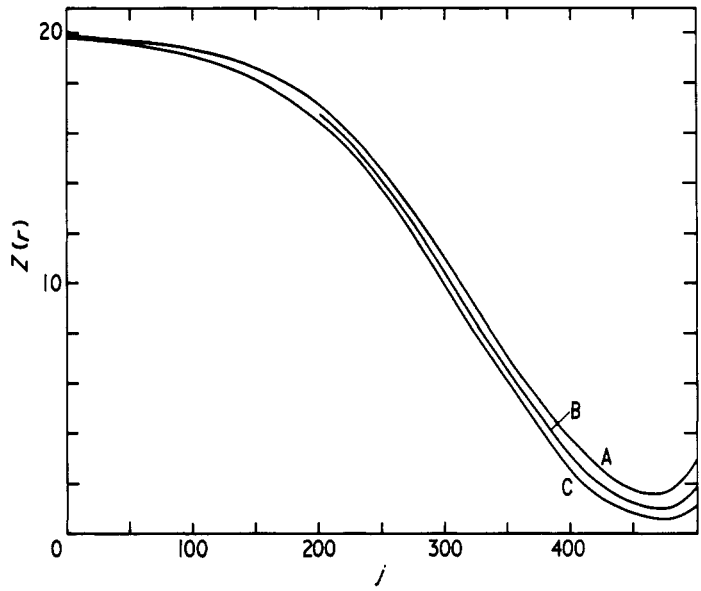

Figure 1. The potential for different values of the exchange term. A $\alpha = 1$; B $\alpha = 0{\cdot}4$, C $\alpha = 0$. The potential is $Z(r)/r$. The values of r in au are given by $r = \exp\{-6{\cdot}125 + (j/64)\}$.

It should be noticed that the potential depends on the lattice constant a through the expansion of the potentials of the neighbouring cells. The potentials shown in figure 1 were computed for the equilibrium value at atmospheric pressure $a = 5{\cdot}57$ Å $= 10{\cdot}5$ au, but were recomputed whenever the lattice constant was changed.

4. The bands

4.1. *Effect of exchange*

The bands along the lines of symmetry are displayed in figures 2 and 3 where the notation of Altmann and Cracknell (1965) is used, as elsewhere in this paper. Figure 2 gives the bands for $\alpha = 0{\cdot}4$, $a = 10{\cdot}5$ au. It can be seen that there is a small overlap between the first and second bands which is due to the fact that the second level at L, LA_{2u}, of energy 0·293 Ryd, lies below the first levels at W and K, WB_2 (0·321 Ryd) and KA_1 (0·308 Ryd) respectively. The W–L overlap, given by the difference of the WB_2 and LA_{2u} eigenvalues, is 0·028 Ryd and the K–L overlap 0·015 Ryd. It was soon found that these overlaps are extremely sensitive to changes in α. For instance, they are much reduced in figure 3, which gives the bands for $\alpha = 0{\cdot}7$, for which the K–L overlap has almost closed down to the value 0·006 Ryd and the main W–L overlap is little more than one half of the previous one, taking the value 0·016 Ryd.

This sensitivity of the results to the value of α is not a new result. In several computations of metallic bands it has been found necessary to take values of $\alpha \neq 1$ in order to obtain

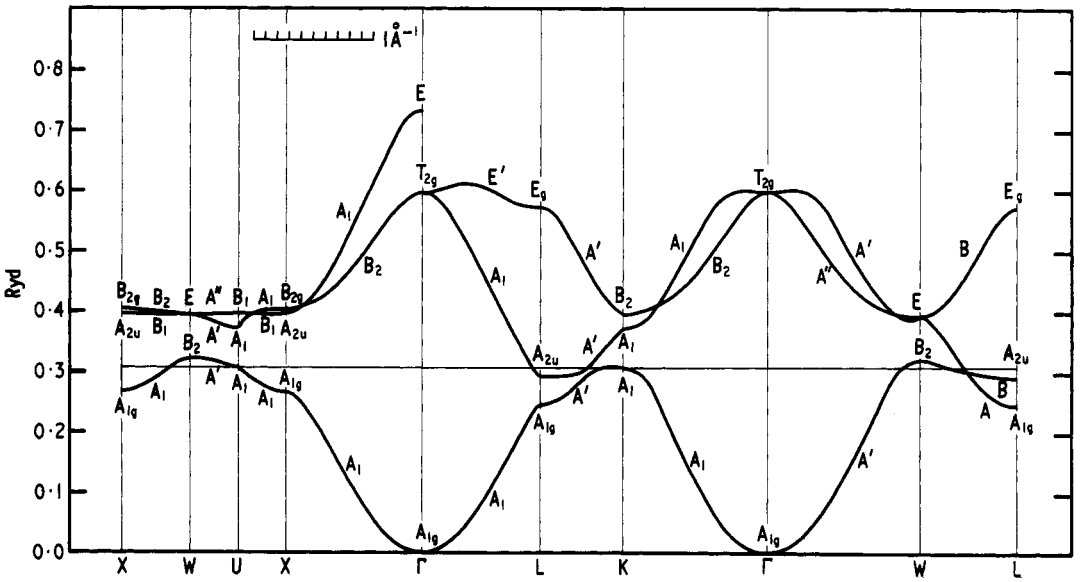

Figure 2. Bands for Ca. $a = 10{\cdot}5$ au, $\alpha = 0{\cdot}4$. The value $E(\Gamma A_{1g})$ used as reference for the energies, is $-0{\cdot}473$ Ryd.

agreement with experiment and a value of α around $\frac{2}{3}$ has often been used. What makes Ca a most interesting case is that for a wide range of α there is no overlap at all between W and L. Thus, it is not here a question that α merely affects the shape of the Fermi surface but rather that, whereas for some values of α one finds holes at W and electrons at L (see figure 2), for others, those surfaces entirely disappear and one is left with no more than an infinitesimal Fermi surface around the line of degeneracy. (See the crossing point of the first and second

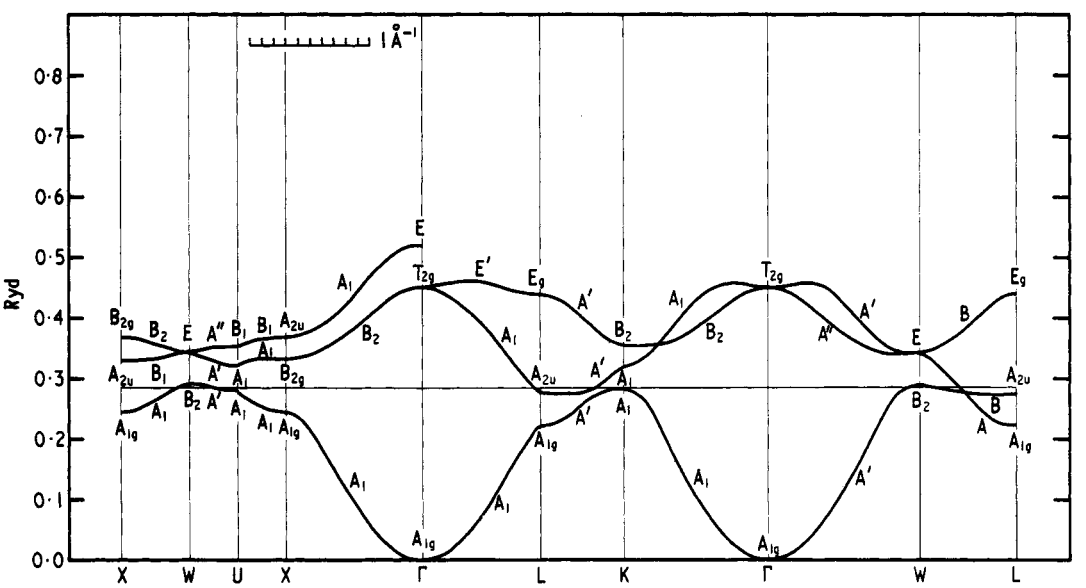

Figure 3. Bands for Ca. $a = 10{\cdot}5$ au, $\alpha = 0{\cdot}7$. $E(\Gamma A_{1g}) = -0{\cdot}696$ Ryd.

bands along LW). This situation is illustrated in figure 4 where the K–L and W–L overlaps are given as a function of α: it follows that there is no overlap at all between the first and second band at these points except in the range $0{\cdot}2 < \alpha < 0{\cdot}75$.

Unfortunately, the evidence from experimental studies of the Fermi surface (see § 6) is not good enough to determine the value of α in the range just mentioned which gives the best agreement with experiment. On the other hand, the study of the behaviour of the bands at high pressure (§ 8) indicates that the overlap should be larger than even the maximum

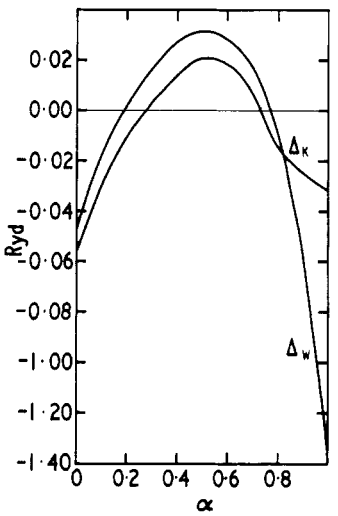

Figure 4. Overlaps as a function of the exchange parameter. $\Delta_K = E(KA_1) - E(LA_{2u})$: $\Delta_W = E(WB_2) - E(LA_{2u})$.

value obtained from figure 4 for $\alpha = 0{\cdot}5$. It is thus probable that the bands should be a little more free-electron-like than any of our Slater-type potentials allows. This shows that a potential such as the one used in figure 3 ($\alpha = 0{\cdot}70$) can be rejected, since it compresses the bands away from the free-electron picture. For instance, it gives a Fermi energy of 0·29 Ryd, smaller than that for $\alpha = 0{\cdot}40$ (0·310 Ryd) and much too far away from the free-electron Fermi energy of 0·344 Ryd.

It follows that the best we can do with a potential of the Slater-type is to take a value of α around $\alpha = 0{\cdot}5$ but, since the difference between the results for $\alpha = 0{\cdot}5$ and $\alpha = 0{\cdot}4$ is not very large, in particular in what concerns the Fermi surface (see § 6), we base the result of our discussion on the values obtained for $\alpha = 0{\cdot}4$. Once we were satisfied that a change to $\alpha = 0{\cdot}5$ would not affect significantly our results, it was considered unnecessary to duplicate the calculations. Also, a more detailed analysis of the potential field conducted in this department, in which exchange and screening are introduced more accurately than by means of the Slater term, provides a potential for which the K–L overlap is much larger than in the present paper and in better agreement with the high-pressure experiments.

4.2. *Discussion of the bands*

A selection of our eigenvalues is compared in table 3 with the results of Vasvári *et al.* and of the free-electron model. In both cases the results are not too far from the free-electron picture, those of Vasvári *et al.* being more free-electron-like than the present calculations.

When our results are compared with those of Vasvári *et al.* it can be seen that except for the second level at Γ our eigenvalues coincide in most cases within 0·03 Ryd. However, in the computations of Vasvári *et al.*, their first level at K goes up with respect to ours by about this amount and the second at L goes down in the same way, thus making their

Table 3. Energy eigenvalues (in Ryd) for Ca

Level	Present work†	Vasvári‡	Free electron
ΓA_{1g} (Γ_1)	0·000	0·000	0·000
ΓT_{2g} (Γ'_{25})	0·600	0·905	1·054
LA_{1g} (L_1)	0·248	0·245	0·263
LA_{2u} L_2)	0·293	0·262	
KA_1 (K_1)	0·308	0·336	
KA_1 (K_1)	0·374	0·394	0·395
KB_2 (K_3)	0·397	0·379	
WB_2 (W'_2)	0·321	0·364	0·438
WE (W_3)	0·395	0·396	
WB_2–LA_{2u}	0·028	0·102	0·175
Fermi energy	0·308	0·339	0·344

† Computed for $\alpha = 0{\cdot}4$, $a = 10{\cdot}5$ au.
‡ Computed by Vasvári *et al.* (1967) and reported by Vasvári (1968).

overlap about 0·07 Ryd larger than ours. It is probable from the discussion of § 8 that the true overlap lies somewhere between ours and that of Vasvári *et al.*

An important difference between the two sets of computations should be noticed: whereas in our calculations the levels at K are, in increasing order of energies, KA_1, KA_1 and KB_2, those for Vasvári *et al.* are KA_1, KB_2, KA_1. The significance of this difference can be appreciated from table 4. Both in our calculations and those of Vasvári *et al.* the first band is heavily hybridized, so that some substantial s contribution must appear in the higher bands. In a fairly free-electron band where sp hybridization is permitted, one would expect the first band to have a large p contribution somewhere at the edge and the corresponding second band, instead, to have there a large s contribution. This is exactly what we find at K and these, except for the similar U points, are the only points for which the symmetry of the second band permits an s contribution. However, the second level at K of Vasvári *et al.*, being KB_2, does not admit of an s contribution. None of the other second levels of Vasvári *et al.*, which are of the same symmetry as ours, can admit an s contribution. It would appear therefore that in the calculations of Vasvári *et al.* the s contribution in the higher bands would be found in the third band at KA_1 (and UA_1) which is somewhat unexpected, unless of course, it appears in the second band at general $\boldsymbol{k}$ vectors. Nevertheless, in most cases, it is the symmetry restrictions at the points of symmetry that determinine the nature of the wave functions of a band, these restrictions propagating by continuity for some distance away from the corresponding symmetry points.

Discussion of the position of the Fermi levels in table 3 will be left until § 6.

Table 4. The wavefunctions. $a = 10{\cdot}5$, $\alpha = 0{\cdot}40$

	First band					Second band				
	Γ A_{1g}	L A_{1g}	K A_1	X A_{1g}	W B_2	Γ T_{2g}	L A_{2u}	K A_1	X A_{2u}	W E
s	100	53	5	22	—	—	—	16	—	—
p	—	—	28	—	27	—	96	17	93	52
d	—	47	64	77	69	96	—	64	—	45
f	—	—	2	—	4	—	4	2	6	2

The figures given in the table are the percentage contribution of each harmonic to the wave functions. A dash means that the contribution vanishes by symmetry. Where the total in any column falls short of 100 there is a detectable contribution to the wave function from $l \geqslant 4$.

4.3. *Core levels*

The calcium core $1s^2\ 2s^2\ 2p^6\ 3s^2\ 3p^6$ has the same configuration as the argon atom, for which Mattheiss (1963) computed the valence bands. Figure 5 shows the 3s and 3p bands for calcium computed for $a = 10{\cdot}5$ and $\alpha = 0{\cdot}4$. For comparison, we also give Mattheiss' eigenvalues for argon in a suitable scale. The correspondence between the calcium and argon bands thus scaled is remarkable. The order and relative position of the eigenvalue at all points of symmetry coincides precisely once the scaling is done. The coincidence of the levels at K is particularly gratifying, on account of the difference at this

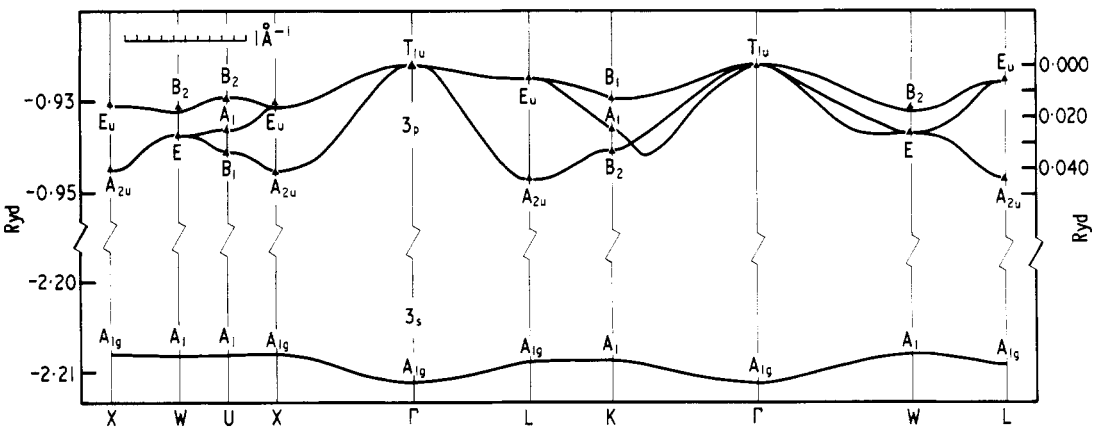

Figure 5. The bands for the core levels of Ca. The energy scale is given on the left: notice that it is broken and that there is a different scale for each set of bands. The triangles correspond to the eigenvalues of the 3p band of argon calculated by Mattheiss, in the scale given on the right of the figure. The energy levels for Ca are given in an energy scale for which $\Gamma A_{1g} = 0$ in figure 2 (its absolute value is $-0{\cdot}473$ ryd). The absolute value of $E(T_{1u})$ for argon is $-1{\cdot}253$ ryd.

point between our results for the conduction band and those of Vasvári *et al.* Not surprisingly, the core bands for calcium are more compact than those for argon. Thus the band widths for calcium are 0·026 Ryd for the 3p band and 0·006 Ryd for the 3s band, whereas the corresponding figures for argon are 0·044 and 0·010 Ryd respectively. The energy difference between the centres of the calcium 3s and 3p bands is 1·254 Ryd, which compares very well with the experimental value 1·3 Ryd for the difference between the calcium atom 3s and 3p levels (Slater 1955).

It should be noticed that the 3p band width is not negligible in comparison with that of the conduction band, being 8·4% of it. Thus, it is possible that the distortion of the 3p core levels might have a small but significant effect on the conduction band.

5. Density of states

The density of states was computed as indicated in § 2 and is shown in figure 6. The computed Fermi energy is 0·310 Ryd (see also § 6) and the corresponding band width of 4·23 eV can be compared with the value of about 7 eV measured by Skinner *et al.* (1954), a result which unfortunately might have been affected by surface contaminations. Also other effects, such as slit width corrections, background, etc. can easily introduce corrections of about 2 eV.

The density of states at the Fermi surface derived from our curve is 13 states/Ryd/atom which leads to a value of the low temperature coefficient of specific heat γ equal to $5{\cdot}5\ 10^{-4}$ cal mole^{-1} deg^{-2}, to be compared with an experimental value of 6·5 in the same units.

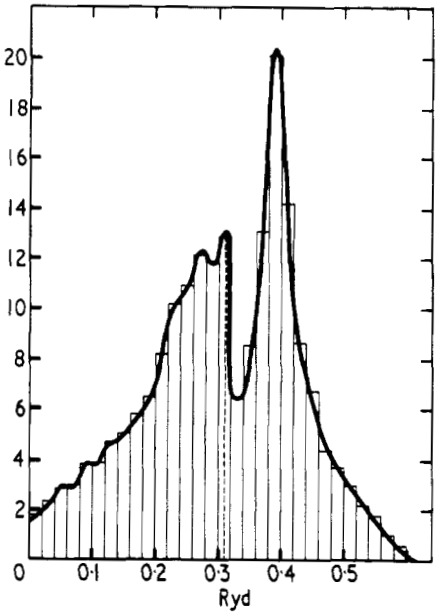

Figure 6. The density of states $n(E)$ in electron states of both spins per rydberg per atom. The broken vertical line is the Fermi energy.

This is an excellent agreement, since the electron phonon interactions should not be large in calcium metal.

6. The Fermi surface

Once the value of the Fermi energy, 0·310 Ryd, was determined from the density of states calculations, the interpolation scheme described in § 2 was used to obtain level

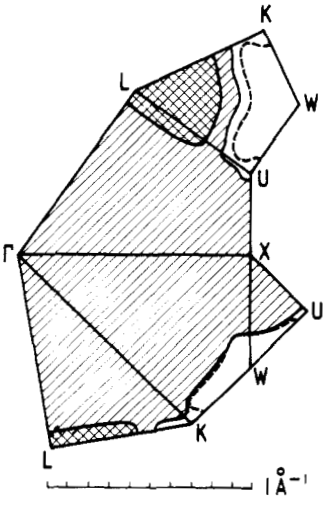

Figure 7. The Fermi surface for $E_F = 0{\cdot}308$ Ryd. Empty areas contain holes and hatched areas electrons. Areas with double hatching indicate pockets of electrons in the second zone. The broken lines given the contour for $E = 0{\cdot}310$ Ryd. where it is significantly different from the contour for $E_F = 0{\cdot}308$ Ryd.

surfaces around this value. Since their shape varies widely in certain regions for variations of 0·002 Ryd in the eigenvalues, direct computation was also employed when necessary. The level surfaces are shown in figures 7 and 8. It can be seen that there are pockets of electrons at L in the second band (saucer). Also, if $E_F = 0{\cdot}310$, the surface of holes in the first band is unconnected, consisting of pockets at W, which, because they have (squashed) tetrahedral symmetry, will be called tetroids.

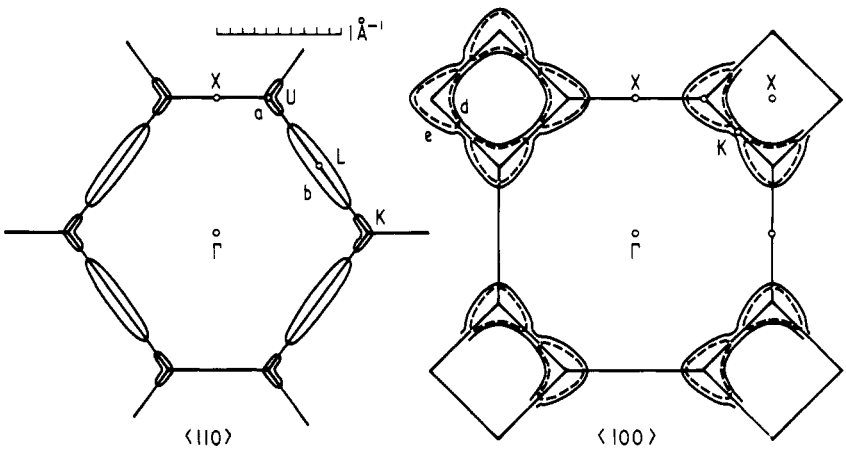

Figure 8. Important sections of the Fermi surface for $E_F = 0{\cdot}308$ Ryd. The broken contour corresponds to $E = 0{\cdot}310$ Ryd.

Once these results are obtained, it must be remembered that the computed value of E_F is not accurate to more than about 0·005 Ryd and that the volume of the pockets of electrons in the second band must equal that of the pockets of holes in the first. There is no guarantee, from the computations of E_F from the density of states, that this equality is verified exactly and the right procedure is to correct the computed E_F until the volumes are properly balanced.

The order of the group of W is 8 and that of Γ 48, whence it follows that the number of tetroids per Brillouin zone is 48/8 = 6. Likewise, the number of saucers is 4, so that the ratio

$$\tau = \text{vol saucer/vol tetroid} = 1{\cdot}5. \tag{1}$$

We found that for $E_F = 0{\cdot}310$ Ryd, $\tau = 2{\cdot}3$, and it was not possible, by exploring the shape of the tetroid in greater detail, to improve on this value. On the other hand, it can be seen from figure 7 that the volume of the tetroid is very sensitive to the value of E_F whereas the saucer is relatively stable. Even a change of 0·001 Ryd to $E_F = 0{\cdot}309$ Ryd affects the shape of the tetroid substantially, making it connected through necks along LK but at some small distance of K. However, even then the volumes are not right and the orbits do not agree with the de Hass–van Alphen results.

For $E_F = 0{\cdot}308$ Ryd the tetroid is connected through flat necks along LK which reach and surround K itself. For this value of E_F, $\tau = 1{\cdot}4$ in acceptable agreement with (1) and the orbits found correlate very well with the de Haas–van Alphen results (see § 7). Hence, we consider this to be the best value of the Fermi energy compatible with our results and conclude that the Fermi surface is most likely to be connected (see figure 10).

The volume of the saucers is 0·080 $Å^{-3}$, leading to the existence of 1·89 electrons/atom in the first band and 0·11 in the second.

6.1. *The computations of Vasvári et al.*

Since Vasvári and Heine (1967) and Vasvári (1968) derive an unconnected Fermi surface from the bands of Vasvári *et al.* (1967), it is desirable to compare their results with ours: we shall show that there is no contradiction but rather, that an erroneous assumption was made in the work of Vasvári *et al.* which, when corrected, should also lead to a connected Fermi surface. Vasvári *et al.* took the value $E_F = 0{\cdot}33$ Ryd (or about 0·34 Ryd if measured from the lowest eigenvalue at Γ) in an attempt to obtain an unconnected Fermi surface (see Vasvári and Heine 1967) and thus, as was previously done by Altmann and Cracknell (1964), explain most simply the small number of periods observed in the de Haas–van Alphen effect. However, in doing so, it appears that these authors failed to verify the fundamental relation (1). An estimate of the volumes of their Fermi surface can easily be obtained. From the bands in figure 1 of Vasvári *et al.* (1967), the semimajor axis of the saucer along LW is $0{\cdot}535$ Å^{-1} and the largest radius of the tetroid, along WU, is $0{\cdot}201$ Å^{-1}. From figure 2 of Vasvári (1968), the semimajor axis of the saucer along L is $0{\cdot}166$ Å^{-1}. Thus, the volume of the saucer can be very well estimated as an ellipsoid and it is $0{\cdot}199$ Å^{-3}. Since this is more than twice the volume of our saucer ($0{\cdot}080$ Å^{-3}), the most favourable hypothesis for Vasvári *et al.* is to take the largest possible volume of the tetroid, which is the sphere of radius equal to the dimension of the tetroid along WU. This gives a volume $0{\cdot}034$ Å^{-3} so that $\tau = 5{\cdot}9$, which is probably a lower bound for τ, since any more realistic estimate of the volume of the tetroid produces values of τ larger than 10. We conclude that the bands given in figure 1 of Vasvári *et al.* are not compatible with the Fermi energy proposed by them. In order to increase the volume of the tetroid and bring down τ to its correct value, the Fermi level has to be brought down by 0·01 Ryd or more so that the holes extend from W to K. It appears to us most unlikely that the bands of Vasvári *et al.* could lead to a Fermi surface which is not connected. This being so, the conclusions derived by these authors about the conductivity of calcium, its high pressure behaviour and the de Haas–van Alphen experiments must be entirely revised; they depend critically on the size and shape of a Fermi surface upon which no reliance can be placed, because the volume of holes is incorrect by a factor that cannot be smaller than 4 and which is likely to be at least 6.

7. The de Haas–van Alphen results

7.1. *Experimental results*

The de Haas–van Alphen effect was observed in calcium by Condon and Marcus (1964). Unfortunately, it turned out that their sample was a microcrystallite rather than a single crystal and this makes the interpretation of their results more difficult. In particular, the crystal orientations measured against external faces (fiduciary orientations) are not necessarily the true ones. Condon and Marcus observed three periods, shown in figure 9, which reproduces one set of their results. In order to facilitate comparison with our theoretical Fermi surface, we shall summarize systematically all the results that appear well established from Condon and Marcus experiments.

(i) The periods observed are $l = 3{\cdot}05\ 10^{-7}$ G^{-1}, $m = 0{\cdot}77\ 10^{-7}$ G^{-1}, $s = 0{\cdot}57\ 10^{-7}$ G^{-1} with fiduciary orientations as in (*a*) of figure 9.

(ii) The angular dependence of l is well established, as shown in figure 9, where the broken line gives the angular dependence of a cross section of a cylindrical surface.

(iii) Period l and s appear together.

(iv) Periods l and m never appear together.

(v) Period l is repeated every 60° when the magnetic field is rotated in the (111) plane. (see figure 4 of Condon and Marcus 1964 or figure 3 of Altmann and Cracknell 1964).

(vi) Period m does not appear when the field is rotated in the (111) plane.

7.2. *Computed orbits and experimental correlation*

The values and orientations of the computed orbits are shown in table 5. Orbit a (figure 8) is the neck orbit of the tetroid at K. Orbit b (figure 8) is the belly orbit of the saucer. Orbit c (figure 10) is a body orbit of the tetroid in a plane whose normal is about 20° off the

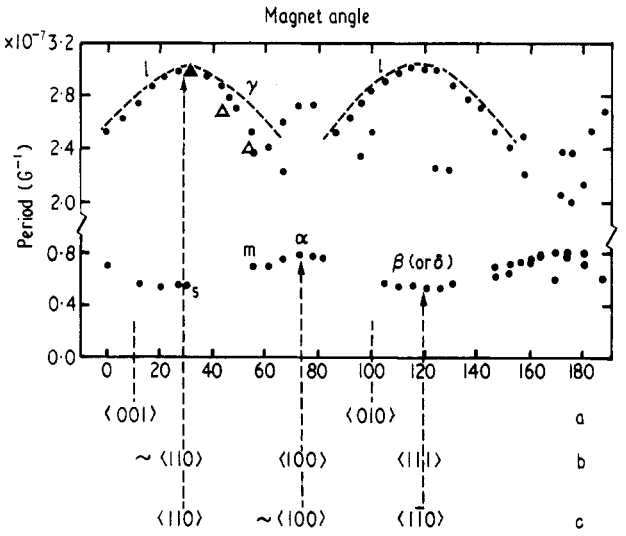

Figure 9. de Haas–van Alphen periods after Condon and Marcus. Magnetic field rotated in the (100) plane: (*a*) fiduciary orientations, (*b*) Condon and Marcus reassignment to fit Harrison's Fermi surface, (*c*) our reassignment.

⟨100⟩ direction. Orbit d (figure 8) is the rim of the ring of tetroids on the square face and orbit e (figure 8) is an extended orbit of the tetroids. Orbits f and g (figure 12) are respectively the rim orbit of the saucer on the hexagonal face and the rim of the teroid ring on the same face. The orientation of these orbits are given in the second column of table 5.

Our interpretation of the experimental results is based on two major assumptions. Condon and Marcus (1964) found three orbits only, whereas we have seven. However, the rim orbit of the saucer, f, is one that must be considered as an established feature of the Fermi surface, since all calculations agree to the extent that this orbit exists and as to its order of magnitude, but it was not observed by Condon and Marcus. It must therefore be assumed that their crystal was too imperfect to allow the observation of an orbit as large as f. Since d, e and g are of the same order of magnitude, the lack of observation of these orbits is understandable.

Table 5. Computed orbits and experimental periods

Orbit	Computed orientation	Period	Experimental Period	Name
a	⟨110⟩	3·8	3·05	*l*
b	⟨110⟩	0·68	0·57	*s*
c	near ⟨100⟩	0·60	0·77	*m*
d	⟨100⟩	0·21		
e	⟨100⟩	0·09		
f	⟨111⟩	0·16		
g	⟨111⟩	0·12		

All periods are in $10^{-7}\,G^{-1}$. The orientations are those of the normal to the plane of the orbit. The name of the period identifies it in figure 9.

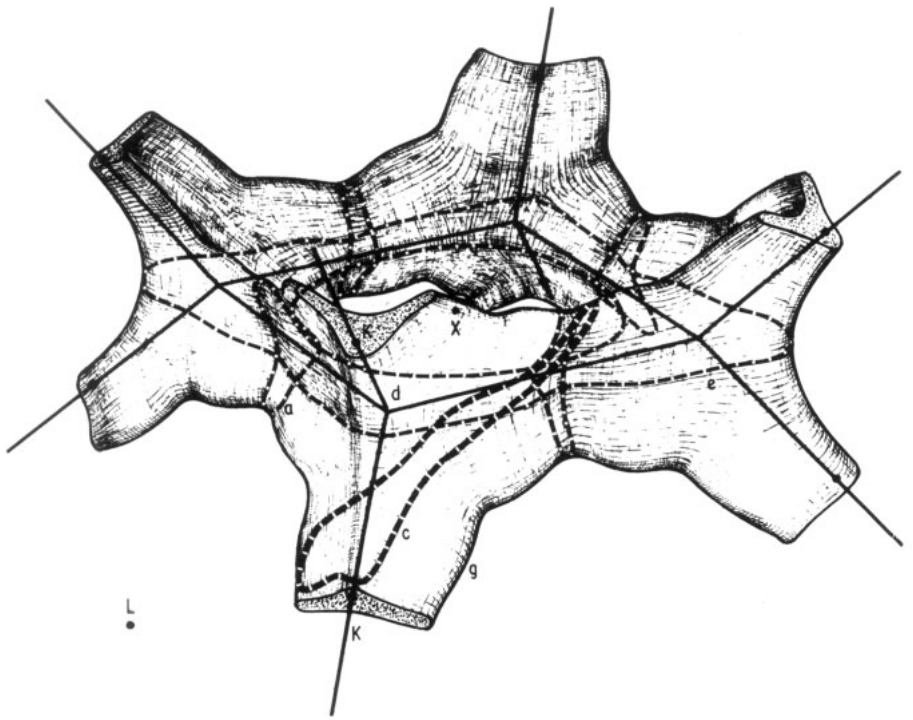

Figure 10. Fermi surface for Ca. The surface shown contains holes in the first band. Four tetroids are shown, connected in a torus around X.

The second major assumption relates to the reinterpretation of the crystal orientations that we must make in order to correlate the remaining three orbits a, b, c with the periods *l*, *s* and *m*. This reinterpretation is given in (*c*) of figure 9 and it can be seen that it is similar to that given by Condon and Marcus, with the advantage that it respects the fact, clear from the figure, that the angle between the peaks of the two *l* periods is fairly exactly 90°.

It can be seen from table 5 that the quantitative agreement between the computed and experimental values of the periods is fair. In fact, considering the sensitivity of the orbits to errors of 0·001 Ryd in the eigenvalues, it would be unrealistic to expect a much better fit.

In order to show the angular dependence of the period *l* in figure 9, we scale the curve so as to get the computed maximum period to coincide with the experimental maximum. The computed points (shown with triangles) agree fairly well with the experimental angular dependence.

The orbits a and b must appear together (see figure 8) as is indeed the case with the periods *l* and *s* that we assign to them (see (iii) of § 7.1.). The neck orbit a must be repeated at intervals of 60° when the field is rotated in the hexagonal face in agreement with the behaviour of of period *l*. (See (v) of § 7.1.).

It can be shown (see figure 10) that the body period of the tetroid, c, disappears when the magnetic field is tilted away from the maximal cross section by 20° or so. This is the case because the tetroids form a torus-like object around X. The orbit c cuts the boundary of the torus but, when it is slightly tilted, it runs into the body of the torus and is replaced by either e or d (see figure 8). Thus, orbit c can only be observed within a small angular range. This agrees with the fact that the period *m* which we assign to c never appears with *l*((v) of § 7.1) and does not appear at all when the field is rotated in the (111) plane ((vi) of § 7.1.)

It can thus be seen that our interpretation accounts satisfactorily for all the experimental results listed in § 7.1.

A comparison with the interpretation of the de Haas–van Alphen experiment given by Vasvári (1968) is hardly necessary, owing to the difficulties mentioned in § 6 about his Fermi surface. It might be mentioned, however, that his proposed interpretation does not account for the vital period *l* and that the predicted values of *s* and *m* are 0·45 and 0·34 10^{-7} G^{-1} respectively (see table 5).

8. High pressure behaviour of Ca

In order to study the high pressure behaviour of Ca we computed the bands as a function of $\omega = V/V_0$, where V and V_0 are the volumes of the unit cell at the pressures P and P_0 (normal) respectively. We show in figure 11 the bands for $\omega = 0{\cdot}86$. Comparison with figure

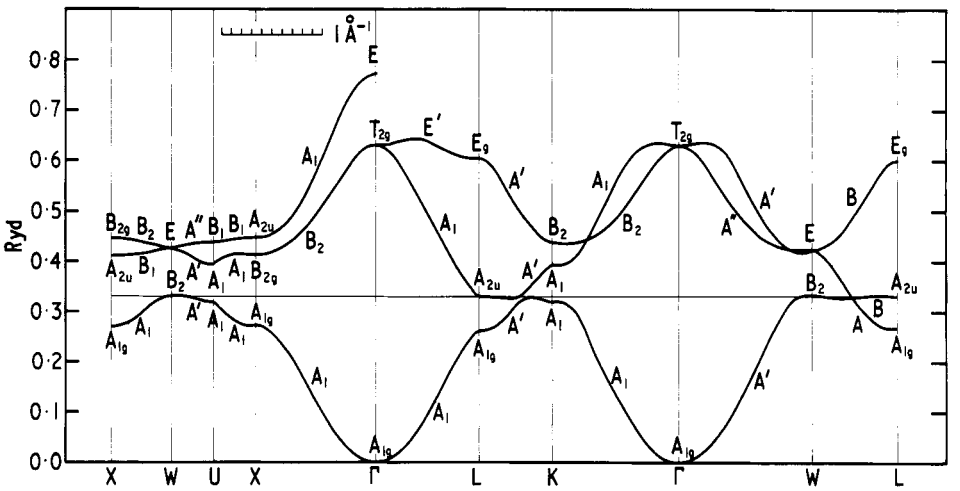

Figure 11. Bands for Ca. $a = 9{\cdot}975$ au, ($\omega = 0{\cdot}86$), $\alpha = 0{\cdot}4$. $E(\Gamma A_{1g}) = -0{\cdot}526$ Ryd.

2 shows that all levels in the first band go up by about 0·01 Ryd, except X which is unchanged. On the other hand, in the second band, L goes up by about three times as much, thus reducing the overlap between L and W to a few thousands of a rydberg. When the wave functions are examined (cf. table 4) it is seen that, on compression, the d contribution is increased throughout by a few percent but the second level at L, which is essentially p, remains exactly unchanged in composition. Thus the rise in energy due to compression is largely compensated by a greater d contribution, except for the second level at L, so that its relative increase of energy is larger.

The Fermi energy for $\omega = 0{\cdot}86$ goes up to 0·33 Ryd and it can be seen at once that the Fermi surface must be much reduced in volume, which is confirmed from figure 12, where the Fermi surface contours on the hexagonal face of the Brillouin zone are given, for comparison, for $\omega = 1$ and $\omega = 0{\cdot}86$. It can be seen from the bands that for $\omega = 0{\cdot}86$ the overlap between KA_1 and LA_{2u} has disappeared, as a result of which K is no longer occupied by holes, which are now concentrated in small pockets around W. It follows that at compression slightly larger than that corresponding to $\omega = 0{\cdot}86$ even the pockets of holes at W will disappear entirely, as well of course as the pockets of electrons at L. At this stage the Fermi surface must become infinitesimal, reduced at most to tiny pockets of holes and electrons along the line of degeneracy that goes through the crossing point of the first and second bands at Q (along LW, see figure 11). That is, the material becomes a semimetal.

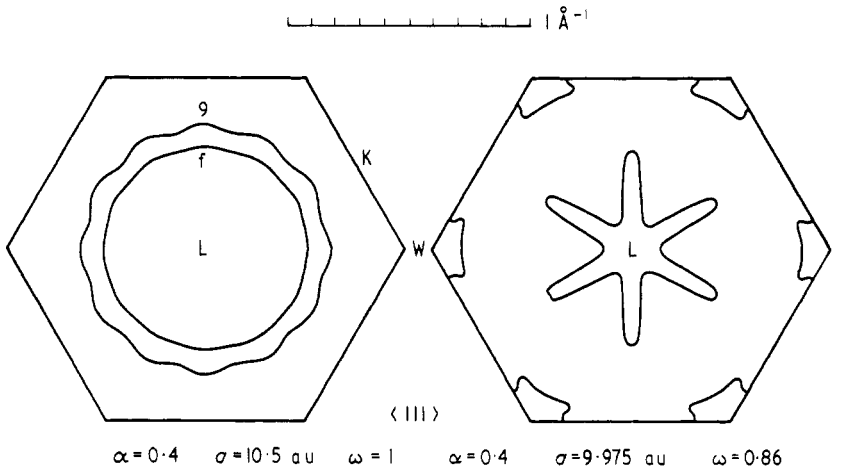

Figure 12. Sections of the Fermi surface for $\omega = 1$ and $\omega = 0{\cdot}86$.

In order to find the value ω' of ω at which the Fermi surface collapses as described, we computed the overlaps $\Delta_W = E(WB_2) - E(LA_{2u})$ and $\Delta_K = E(KA_1) - E(LA_{2u})$ as a function of ω, which are plotted in figure 13. The negative values of Δ in the figure correspond to energy gaps, and it follows from figure 13 that, as explained before, the holes recede first from K and that at $\omega = 0{\cdot}84$ the overlap at W disappears. This is therefore the value ω' at which the Fermi surface collapses.

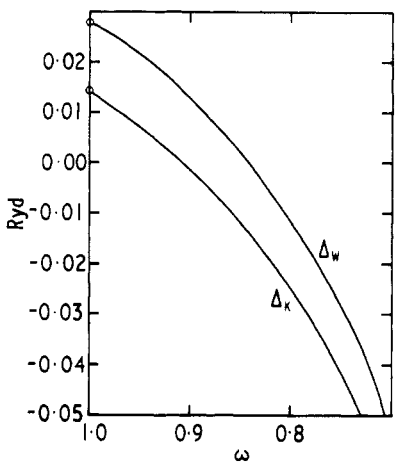

Figure 13. Overlaps as a function of ω. $\Delta_K = E(KA_1) - E(LA_{2u})$; $\Delta_W = E(WB_2) - E(LA_{2u})$.

Stager and Drickamer (1963) studied the behaviour of Ca at high pressure. As summarized by Drickamer (1965) a sluggish transition commences at 140 kbar to a 'semiconducting' phase, which is completed at 300 kbar. In this context, 'semiconductor' merely means that the resistance ρ decreases with temperature. We can distinguish four regions in the curves given by Drickamer (1965, figure 98). Two regions, α, from normal pressure up to about 140 kbar. and δ. above 400 kbar. can be considered typically metallic ($\rho_{296K} > \rho_{77K}$).

Before δ, from 300 to 400 kbar, there is a region γ which is typically 'semiconducting' ($\rho_{296K} < \rho_{77K}$). Finally, between γ and the initial metallic region α there is a region β (from about 140 kbar to 300 kbar) that cannot by any means be considered typically metallic: ρ_{296K} is hardly different from ρ_{77K}. Since a finite size of the Fermi surface must lead to normal metallic behaviour, as in the first region α, we suggest, as Altmann and Cracknell (1964) did, that the onset of region β at 140 kbar corresponds to the pressure at which the Fermi surface vanishes, – that is, to the value $\omega' = 0{\cdot}84$ computed above.

In order to express ω as a function of the pressure we used Birch's equation of state as given by Brush (1967), after fitting the experimental values of Bridgman (1942) up to 100 kbar. We obtained for $\omega' = 0{\cdot}84$ the pressure of 35 kbar, to be compared with 140 kbar. The latter value corresponds to $\omega = 0{\cdot}67$, so that our value of ω' is off by about 20%. This would indicate that the value of Δ_W for $\omega = 1$ is far too small and since the value we started from was the largest given by a Slater potential, it suggests that another type of potential field is required. However, the present calculations reproduce qualitatively the right type of behaviour.

Acknowledgment

One of us (SLA) wishes to acknowledge a discussion with Dr B. Vasvári about the electron imbalance in the calculations of Vasvári *et al.* ARH and RGB gratefully acknowledge Science Research Council studentships.

References

ALTMANN, S. L., and BRADLEY, C. J., 1965, *Proc. Phys. Soc.*, **86**, 915–31.
ALTMANN, S. L., and CRACKNELL, A. P., 1964, *Proc. Phys. Soc.*, **84**, 761–5.
ALTMANN, S. L., and CRACKNELL, A. P., 1965, *Rev. mod. Phys.*, **37**, 19–32.
ALTMANN, S. L., DAVIES, B. L., and HARFORD, A. R., 1968, *J. Phys.* C: *Solid St. Phys.*, **1**, 1633–36.
BRIDGMAN, P. W., 1942, *Proc. Am. Acad. Arts Sci.*, **74**, 425–40.
BRUSH, S. G., 1967, *Progress in High Temperature Physics and Chemistry*, ed. C. A. Rouse (Oxford: Pergamon), **1**, 1–137.
CONDON, J. H., and MARCUS, J. A., 1964, *Phys. Rev.*, **134**, A446–52.
CRACKNELL, A. P., 1964, *PhD Thesis*, University of Oxford.
DRICKAMER, H. G., 1965, *Solid St. Phys.*, **17**, 1–133.
LOUCKS, T., 1967, *Augmented Plane Wave Method* (New York: Benjamin).
MATTHEISS, L. F., 1964, *Phys. Rev.*, **133**, A1399–403.
SKINNER, H. W. B., BULLEN, T. G., and JOHNSTON, J. E., 1954, *Phil. Mag.*, **45**, 1070–80.
SLATER, J. C., 1955, *Phys. Rev.*, **98**, 1039–45.
STAGER, R. A., and DRICKAMER, H. G., 1963, *Phys. Rev.*, **131**, 2524–7.
VASVÁRI, B., ANIMALU, A. O. E., and HEINE, V., 1967, *Phys. Rev.*, **154**, 535–9.
VASVÁRI, B., and HEINE, V., 1967, *Phil. Mag.*, **15**, 731–8.
VASVÁRI, B., 1968, *Rev. mod. Phys.*, **40**, 776–81.